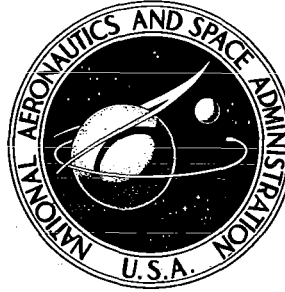


N70-38790

# CASE FILE COPY

NASA TECHNICAL  
MEMORANDUM



NASA TM X-2049

NASA TM X-2049

## AERODYNAMIC CHARACTERISTICS OF A FIXED-WING MANNED SPACE SHUTTLE CONCEPT AT A MACH NUMBER OF 6.0

*by David R. Stone*

*Langley Research Center  
Hampton, Va. 23365*



1. Report No. <b>NASA TM X-2049</b>		2. Government Accession No.		3. Recipient's Catalog No.	
4. Title and Subtitle <b>AERODYNAMIC CHARACTERISTICS OF A FIXED-WING MANNED SPACE SHUTTLE CONCEPT AT A MACH NUMBER OF 6.0</b>				5. Report Date <b>September 1970</b>	
				6. Performing Organization Code	
7. Author(s) <b>David R. Stone</b>				8. Performing Organization Report No. <b>L-7234</b>	
9. Performing Organization Name and Address <b>NASA Langley Research Center Hampton, Va. 23365</b>				10. Work Unit No. <b>124-64-02-05</b>	
				11. Contract or Grant No.	
12. Sponsoring Agency Name and Address <b>National Aeronautics and Space Administration Washington, D.C. 20546</b>				13. Type of Report and Period Covered <b>Technical Memorandum</b>	
				14. Sponsoring Agency Code	
15. Supplementary Notes					
16. Abstract  <p>The longitudinal, directional, and lateral stability and control characteristics of the orbiter stage of a two-stage space shuttle concept proposed by the NASA Manned Spacecraft Center have been determined. Longitudinal data were obtained at angles of attack from <math>-5^{\circ}</math> to <math>60^{\circ}</math>, and lateral and directional data were obtained at sideslip angles of <math>0^{\circ}</math>, <math>-2^{\circ}</math>, and <math>-5^{\circ}</math> over this angle-of-attack range. The tests were conducted at a Mach number of 6.0 and a free-stream Reynolds number of <math>1.24 \times 10^7</math> per meter (<math>3.79 \times 10^6</math> per ft).</p>					
17. Key Words (Suggested by Author(s))  Fixed-wing space shuttle Space vehicles Hypersonic aerodynamic characteristics				18. Distribution Statement  Unclassified - Unlimited	
19. Security Classif. (of this report) <b>Unclassified</b>		20. Security Classif. (of this page) <b>Unclassified</b>		21. No. of Pages <b>26</b>	
				22. Price* <b>\$3.00</b>	

\*For sale by the Clearinghouse for Federal Scientific and Technical Information  
Springfield, Virginia 22151

# AERODYNAMIC CHARACTERISTICS OF A FIXED-WING MANNED SPACE SHUTTLE CONCEPT AT A MACH NUMBER OF 6.0

By David R. Stone  
Langley Research Center

## SUMMARY

The longitudinal, directional, and lateral stability and control characteristics of the orbiter stage of a two-stage space shuttle concept proposed by the NASA Manned Spacecraft Center have been determined at a Mach number of 6.0 and a free-stream Reynolds number of  $1.24 \times 10^7$  per meter ( $3.79 \times 10^6$  per ft). Longitudinal data were obtained at angles of attack from  $-5^\circ$  to  $60^\circ$ , and lateral and directional data were obtained at sideslip angles of  $0^\circ$ ,  $-2^\circ$ , and  $-5^\circ$  over this angle-of-attack range.

The results of this investigation indicate that for the moment reference center at 25 percent of the mean aerodynamic chord (53.48 percent of body length), the configuration trims near the maximum lift coefficient at an angle of attack of about  $48^\circ$  with the maximum allowable elevator deflection of  $-40^\circ$ , and obtains a trim lift coefficient of 2.05 and a trim lift-drag ratio of 0.78. A shift in the center of gravity of approximately 5 percent of the mean aerodynamic chord (0.54 percent of body length) rearward would trim the configuration near an angle of attack of  $60^\circ$  for the present test conditions. The two sting arrangements used had almost negligible effects on the longitudinal forces and moments and only small effects on lateral and directional stability characteristics. The addition of the wing did not change the lift-drag ratio of the basic body shape for angles of attack greater than that for maximum lift-drag ratio. Consequently, the vehicle could be operated at high angles of attack as a fixed-wing or a variable-wing configuration with about the same lift-drag ratio for both configurations. Modified Newtonian theory, in general, underpredicted the forces due to the wing and horizontal tail, and overpredicted the trim angle of attack for the complete configuration with negative elevator deflections.

## INTRODUCTION

Considerable emphasis is currently focused on the development of reusable space transportation systems which offer potential for transportation of large payloads from and to earth. One such concept proposed by the NASA Manned Spacecraft Center is a two-stage, all-reusable manned space shuttle with conventional horizontal-landing capability. Both stages consist of a blunted lifting body with a modified trapezoidal cross

section and a fixed low wing and horizontal tail. The wing has an aspect ratio of 6.95 with a leading-edge sweep of  $15^\circ$  and a dihedral of  $7^\circ$ . The entry mode for the orbiter is considered to be at an angle of attack of approximately  $60^\circ$ , this attitude being maintained until subsonic Mach numbers are achieved. The vehicle is then considered to be rotated by means of aerodynamic controls and reaction controls to attitudes suitable for landing. Reference 1 presented low-subsonic aerodynamic data for an early version of this concept. A later version of the orbiter stage, presented herein, contains design changes as a result of the subsonic tests. The fuselage was made less blunt, the tail sweep angle was reduced to give more tail lift, and the fuselage cross-sectional shape was modified to give better cross-flow characteristics.

The purpose of this investigation is to present the longitudinal, directional, and lateral stability and control characteristics at a Mach number of 6.0 of the later version of the orbiter stage of the two-stage space shuttle conceptual design proposed by the NASA Manned Spacecraft Center. The present investigation was conducted in the Langley 20-inch Mach 6 tunnel. The tests were conducted at angles of attack from  $-5^\circ$  to  $60^\circ$  and at a Reynolds number of  $1.24 \times 10^7$  per meter ( $3.79 \times 10^6$  per ft).

## SYMBOLS

The data for the present investigation are referred to the body-axis system except for the lift and drag coefficients, which are referred to the stability-axis system. The center of moments, unless otherwise specified, is located 1.090 cm above the reference axis at 25 percent of the wing mean aerodynamic chord (53.48 percent of the body length). All coefficients are based on wing planform area, mean aerodynamic chord, and wing span.

b	wing span, 17.65 cm
$C_D$	drag coefficient, $\frac{\text{Drag}}{q_\infty S}$
$C_L$	lift coefficient, $\frac{\text{Lift}}{q_\infty S}$
$C_l$	rolling-moment coefficient, $\frac{\text{Rolling moment}}{q_\infty S b}$
$C_{l\beta}$	effective dihedral parameter at $\beta = 0^\circ$ , $\frac{\Delta C_l}{\Delta \beta}$ , per degree
$C_m$	pitching-moment coefficient, $\frac{\text{Pitching moment}}{q_\infty S \bar{c}}$
$\frac{\partial C_m}{\partial C_N}$	rate of change of pitching moment with normal-force coefficient



$C_N$	normal-force coefficient, $\frac{\text{Normal force}}{q_\infty S}$
$C_n$	yawing-moment coefficient, $\frac{\text{Yawing moment}}{q_\infty S b}$
$C_{n\beta}$	directional stability parameter at $\beta = 0^\circ$ , $\frac{\Delta C_n}{\Delta \beta}$ , per degree
$C_p$	pressure coefficient, $\frac{p - p_\infty}{q_\infty}$
$C_Y$	side-force coefficient, $\frac{\text{Side force}}{q_\infty S}$
$C_{Y\beta}$	side-force stability parameter at $\beta = 0^\circ$ , $\frac{\Delta C_Y}{\Delta \beta}$ , per degree
$c$	wing chord
$\bar{c}$	mean aerodynamic chord of wing, 2.73 cm
$L/D$	lift-drag ratio
$M$	Mach number
$p$	static pressure
$q$	dynamic pressure
$S$	total wing area including area within body, 44.84 cm <sup>2</sup>
$X, Y, Z$	reference axes
$x$	distance along airfoil chord line from leading edge
$x_{cg}$	moment reference center measured from leading edge of mean aerodynamic chord along reference axis
$x_{cp}$	location of center of pressure measured from leading edge of mean aerodynamic chord along reference axis
$y$	vertical distance from airfoil chord line
$\alpha$	angle of attack, deg

$\beta$             angle of sideslip, deg

$\delta_e$            elevator deflection (negative for trailing edge up), deg

Subscripts:

max           maximum

t               stagnation

$\infty$            free stream

Model component designations:

$B_1$            fuselage

$H_6$            horizontal tail

$V_3$            vertical tail

$W_2$            wing

Subscripts on model components refer to nomenclature used in the NASA Manned Spacecraft Center design evolution.

## DESCRIPTION OF MODEL

The vehicle tested was an approximate 0.00725-scale model based on the August 1969 revised baseline orbiter for the two-stage manned space shuttle concept originated by the NASA Manned Spacecraft Center. Details of the model tested are shown in figure 1. The wing had a leading-edge sweep of  $15^\circ$ . The concept as proposed by the NASA Manned Spacecraft Center had a sweep angle of  $14^\circ$ ; however, when the model was constructed, the wing was inadvertently made with a sweep angle of  $15^\circ$ . Photographs of the model installed in the Langley 20-inch Mach 6 tunnel using both a straight sting and a  $60^\circ$  bent sting are presented in figure 2. A portion of the vertical tail and body were removed to allow clearance for the  $60^\circ$  bent sting tests. (See fig. 2(c).) The projected area of the vertical tail for both sting arrangements is given in table I. Elevator deflection was varied from  $0^\circ$  to  $-40^\circ$  which was the maximum allowable negative deflection that would permit adequate clearance of the rocket nozzles. Data were also obtained with an elevator deflected at  $-40^\circ$  with a part removed in the area of the fuselage base

when the straight sting was used. (See fig. 1.) Geometric characteristics of the model are presented in table I.

## APPARATUS AND METHODS

### Tunnel

The test program was conducted in the Langley 20-inch Mach 6 tunnel. The wind tunnel is of the blowdown type, and exhausts through a variable second minimum either to a 3200-cubic-meter vacuum sphere or to the atmosphere with the aid of an annular ejector. The Mach 6.0 nozzle is two-dimensional and contoured, and can be operated at stagnation pressures of 3 to 35 atmospheres (1 atmosphere = 101.325 kN/m<sup>2</sup>) and stagnation temperatures to 556° K. A calibration of the test core (approximately 41 cm × 41 cm) indicates a nominal Mach number of  $6.0 \pm 0.02$ . A more detailed description of this tunnel is given in reference 2.

### Test Conditions and Methods

The tests were conducted at an average stagnation pressure of 1.48 MN/m<sup>2</sup> (215 psia) and a stagnation temperature of 478° K (400° F). The corresponding free-stream Reynolds number was  $1.24 \times 10^7$  per meter ( $3.79 \times 10^6$  per ft). Six-component force and moment data were obtained with the straight sting for an angle-of-attack range from -5° to 55° and with the 60° bent sting from 26° to 60°. For all tests, force and moment data were obtained at angles of sideslip of 0°, -2°, and -5°. Elevator deflection was varied from 0° to -40°.

Force and moment data were obtained by use of a six-component strain-gage balance housed inside the model. Angles of sideslip were obtained by offsetting the model support system to the desired angle; thus, the data were obtained at an essentially constant sideslip angle over the angle-of-attack range. The true angles of attack and sideslip were set optically by the use of a point source of light and a small lens-prism mounted on the model. The image of the light source was reflected by the prism and focused by the lens onto a calibrated chart. Straight-line slopes between the basic data at sideslip angles of 0° to -5° were used to obtain the lateral and directional stability parameters. The data at -2° sideslip were used to verify the linearity of the slopes. Model base pressures were measured during each test, and the axial-force component was adjusted to correspond to a base pressure equal to the free-stream static pressure. The average of two base-pressure tubes, one on the top and one on the bottom of the sting, was used for all tests.

### Accuracy

On the basis of accuracy in balance calibration, zero shift of the balance during tests, computer readout, dynamic pressure, and pressure transducer accuracy, the

probable uncertainties in the force and moment coefficients are estimated by the method of least squares to be as follows:

$C_D$	±0.01
$C_L$	±0.02
$C_{l_\beta}$	±0.0004
$C_{n_\beta}$	±0.0006
$C_{Y_\beta}$	±0.0035
$L/D$	±0.1
$C_m$	±0.02

The accuracy of the angles of attack and sideslip is estimated to be  $\pm 0.10^\circ$  and the free-stream Mach number is estimated to be accurate to  $\pm 0.02$ .

## RESULTS AND DISCUSSION

The results of this experimental investigation are presented in figures 3 to 8. An examination of the shock structure for  $\alpha = 54.2^\circ$  indicates a bulge in the basic body shock caused by the addition of the wing. (See fig. 3(b).) The addition of the wing (fig. 3(d)) also caused a change in the shock structure in the area of the horizontal tail from that observed with the wing removed (fig. 3(c)). These types of component interactions can result in stability problems. (See, for example, ref. 3.) Since complex flow fields of this type are extremely sensitive to model attitude and free-stream conditions, more detailed investigations will be required.

Plots comparing the effects of sting arrangement, elevator deflections, center-of-gravity location, and component contribution to the aerodynamic characteristics are presented in figures 4 to 6. Also, a comparison of the experimental data with analytical estimates from a computer program is presented in figures 7 and 8.

Because of the preliminary nature of the configuration investigated, a detailed analysis of the data has been omitted from this paper; however, a few areas of apparent interest are discussed briefly.

### Aerodynamic Characteristics

A comparison of the aerodynamic characteristics presented in figures 4 and 5 indicates that sting arrangement (compare figs. 2(a) and 2(c)) had an almost negligible effect on the longitudinal forces and moments and had only a small effect on lateral and directional stability characteristics. In particular, the pitching-moment coefficients were in excellent agreement for the common elevator deflections tested on both sting-support arrangements.

For the specified moment reference center ( $x_{cg}/\bar{c} = 0.25$ ), figure 6 indicates that the configuration trims fairly close to  $C_{L,max}$  for the maximum elevator deflection of  $-40^\circ$ ; thus, a trim  $C_L$  of 2.05, a trim  $L/D$  of 0.78, and a trim angle of attack of  $48^\circ$  for this elevator deflection result. Mission considerations have indicated a desire for operation with fixed controls at a higher trim angle of attack ( $\alpha = 60^\circ$ ) throughout the hypersonic-supersonic part of entry. Removal of the part of the elevator directly behind the fuselage base, as indicated in figure 5, increased the trim angle of attack beyond  $60^\circ$  because of a decrease in the static stability level of the configuration at these angles of attack. Consequently, either a smaller horizontal tail, an increased percentage of elevator area relative to the total horizontal-tail area, or a shift in center-of-gravity location could trim the configuration at  $\alpha = 60^\circ$ . Figure 6 indicates that a shift of the center of gravity of approximately 5 percent of  $\bar{c}$  rearward would be sufficient to trim near  $\alpha = 60^\circ$ . Either of these methods would probably produce approximately the same value of  $C_L$  at  $\alpha = 60^\circ$ . (See figs. 5(a) and 6.) Prior to any changes, trim conditions with the present tail-elevator combination should be evaluated experimentally at higher Mach numbers. Secondly, any modifications to achieve trim at  $\alpha = 60^\circ$  must not degrade the subsonic stability and performance.

The vehicle had positive effective dihedral and was statically directionally stable at the design trim point of  $\alpha = 60^\circ$ . (See figs. 5(c) and 6.) It developed a static directional instability below  $\alpha \approx 53^\circ$ ; however, separate studies (unpublished) conducted at both NASA Manned Spacecraft Center and Langley Research Center indicate that the magnitudes of the effective dihedral parameter and vehicle inertias are sufficient to maintain directional stability down to  $\alpha \approx 40^\circ$ .

Figure 7 contains the longitudinal, directional, and lateral stability data for the component buildup with zero elevator deflection angle. The individual components increased the  $C_L$  and  $C_D$  of the configuration by an equal factor for angles of attack greater than that for  $(L/D)_{max}$ ; therefore, no appreciable change was apparent in untrimmed  $L/D$ . Consequently, the vehicle could be operated as a fixed-wing or a variable-wing configuration and would have about the same value of  $L/D$  for both configurations.

## Comparison of Analytical and Experimental

### Aerodynamic Characteristics

A limited comparison is made of the present experimental data with analytical longitudinal, directional, and lateral stability and control characteristics by use of the computer program of references 4 and 5. For the calculation of pressure forces in compression regions, modified Newtonian theory ( $C_{p,t} = 1.818$ ) was used; in expansion regions  $C_p$  was assumed to be zero. Laminar skin-friction calculations assuming adiabatic wall conditions were made according to the method outlined in reference 4 by using Eckert's

reference-temperature (T') method. (See ref. 6.) A comparison of the computer program results with wind-tunnel data for the component buildup is presented in figure 7. Longitudinal force characteristics of the body alone were predicted reasonably well; however, the incremental forces due to the wing and horizontal tail were generally underpredicted. The good agreement of pitching moment for the complete configuration with the theory was fortuitous since the theory failed to predict the incremental contribution of the components. The trim angle of attack for the complete configuration with negative elevator deflections was significantly overpredicted, as indicated in figure 8.

## CONCLUSIONS

An investigation was conducted in the Langley 20-inch Mach 6 tunnel to determine the hypersonic aerodynamic characteristics of the orbiter stage of a two-stage space shuttle concept proposed by the NASA Manned Spacecraft Center. The tests were conducted at angles of attack from about  $-5^{\circ}$  to  $60^{\circ}$  to examine the longitudinal performance and at sideslip angles to  $-5^{\circ}$  and elevator deflections to  $-40^{\circ}$  to obtain static directional and lateral stability and control characteristics. The tests were conducted at a Mach number of 6.0 and a free-stream Reynolds number of  $1.24 \times 10^7$  per meter ( $3.79 \times 10^6$  per ft). Results of the investigation indicate the following conclusions:

1. For the moment reference center at 25 percent of the mean aerodynamic chord (53.48 percent of body length), the configuration trims near the maximum lift coefficient at an angle of attack of about  $48^{\circ}$  with the maximum allowable elevator deflection of  $-40^{\circ}$ ; a trim lift coefficient of 2.05 and a trim lift-drag ratio of 0.78 result.

2. A shift in the center of gravity of approximately 5 percent of the mean aerodynamic chord (0.54 percent of the body length) rearward would trim the configuration near an angle of attack of  $60^{\circ}$  for the present test conditions.

3. Sting arrangement had an almost negligible effect on the longitudinal forces and moments and had only a small effect on lateral and directional stability characteristics.

4. The addition of the wing did not change the lift-drag ratio of the basic body shape for angles of attack greater than that for maximum lift-drag ratio. Consequently, the vehicle could be operated at high angles of attack as a fixed-wing or a variable-wing configuration with about the same lift-drag ratio for both configurations.

5. Modified Newtonian theory, in general, underpredicted the forces due to the wing and horizontal tail, and overpredicted the trim angle of attack for the complete configuration with negative elevator deflections.

Langley Research Center,  
National Aeronautics and Space Administration,  
Hampton, Va., June 25, 1970.

## REFERENCES

1. Decker, John P.; and Spencer, Bernard, Jr.: Low-Subsonic Aerodynamic Characteristics of a Model of a Fixed-Wing Space Shuttle Concept at Angles of Attack to  $76^{\circ}$ . NASA TM X-1996, 1970.
2. Schaefer, William T., Jr.: Characteristics of Major Active Wind Tunnels at the Langley Research Center. NASA TM X-1130, 1965.
3. Fitzgerald, Paul E., Jr.: On the Influence of Secondary Waves From the Intersection of Shocks of the Same Family. J. Aerosp. Sci. (Readers' Forum), vol. 29, no. 6, June 1962, pp. 755-756.
4. Gentry, Arvel E.: Hypersonic Arbitrary-Body Aerodynamic Computer Program. Vol. I - User's Manual. Rep. DAC 56080 (Air Force Contract No. F33615 67 C 1008), Douglas Aircraft Co., Mar. 1967. (Available from DDC as AD817158.)
5. Gentry, Arvel E.: Hypersonic Arbitrary-Body Aerodynamic Computer Program. Vol. II - Program Formulation and Listings. Rep. DAC 56080 (Air Force Contract No. F33615 67 C 1008), Douglas Aircraft Co., Mar. 1967. (Available from DDC as AD817159.)
6. Eckert, E. R. G.: Engineering Relations for Friction and Heat Transfer to Surfaces in High Velocity Flow. J. Aeronaut. Sci. (Readers' Forum), vol. 22, no. 8, Aug. 1955, pp. 585-587.

TABLE I.- GEOMETRIC CHARACTERISTICS OF MODEL

Wing, W<sub>2</sub>:

Aspect ratio . . . . .	6.95
Span . . . . .	17.65 cm (6.95 in.)
Planform area, total . . . . .	44.84 cm <sup>2</sup> (6.95 in <sup>2</sup> )
Planform area, exposed . . . . .	30.32 cm <sup>2</sup> (4.70 in <sup>2</sup> )
Root chord at fuselage center line . . . . .	3.75 cm (1.48 in.)
Tip chord . . . . .	1.33 cm (0.53 in.)
Mean aerodynamic chord . . . . .	2.73 cm (1.08 in.)
Airfoil section, root . . . . .	NACA 0014-64
Airfoil section, tip . . . . .	NACA 0010-64
Leading-edge sweep angle, deg . . . . .	15
Taper ratio . . . . .	0.356

Fuselage, B<sub>1</sub>:

Length . . . . .	25.40 cm (10.00 in.)
Base area used in base-pressure correction . . . . .	4.79 cm <sup>2</sup> (0.74 in <sup>2</sup> )
Planform area . . . . .	93.29 cm <sup>2</sup> (14.46 in <sup>2</sup> )

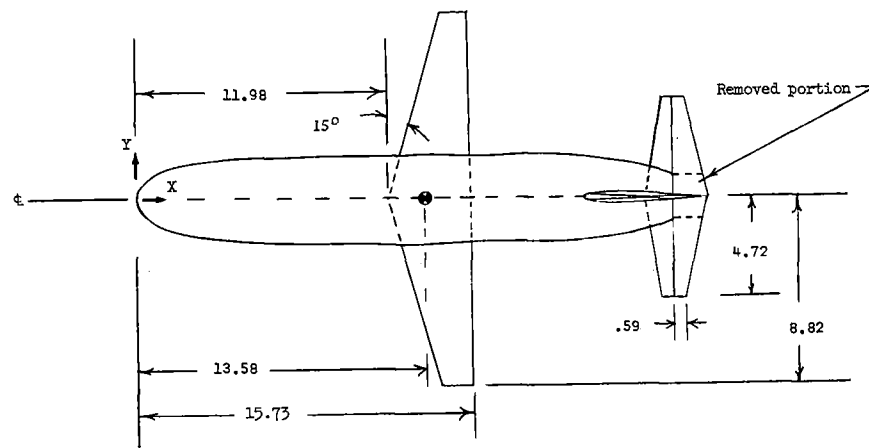
Horizontal tail, H<sub>6</sub>:

Planform area . . . . .	19.04 cm <sup>2</sup> (2.95 in <sup>2</sup> )
Airfoil section . . . . .	NACA 0012-64
Aspect ratio . . . . .	1.26
Elevator planform area . . . . .	10.65 cm <sup>2</sup> (1.65 in <sup>2</sup> )
Elevator planform area, removed section . . . . .	7.36 cm <sup>2</sup> (1.14 in <sup>2</sup> )

Vertical tail, V<sub>3</sub>:

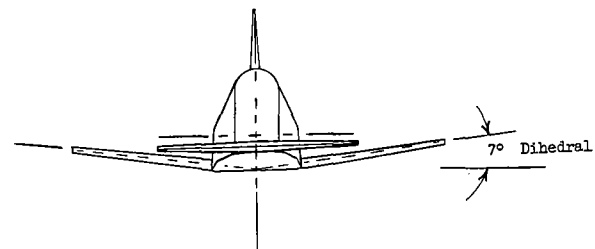
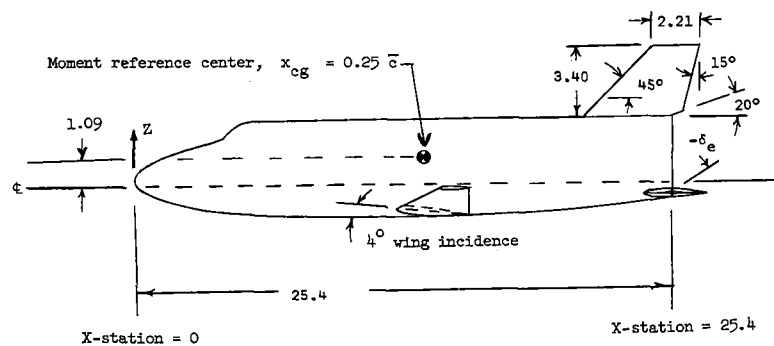
Projected area . . . . .	11.86 cm <sup>2</sup> (1.84 in <sup>2</sup> )
Projected area, 60° bent sting tests . . . . .	10.68 cm <sup>2</sup> (1.66 in <sup>2</sup> )
Airfoil section . . . . .	NACA 0012-64





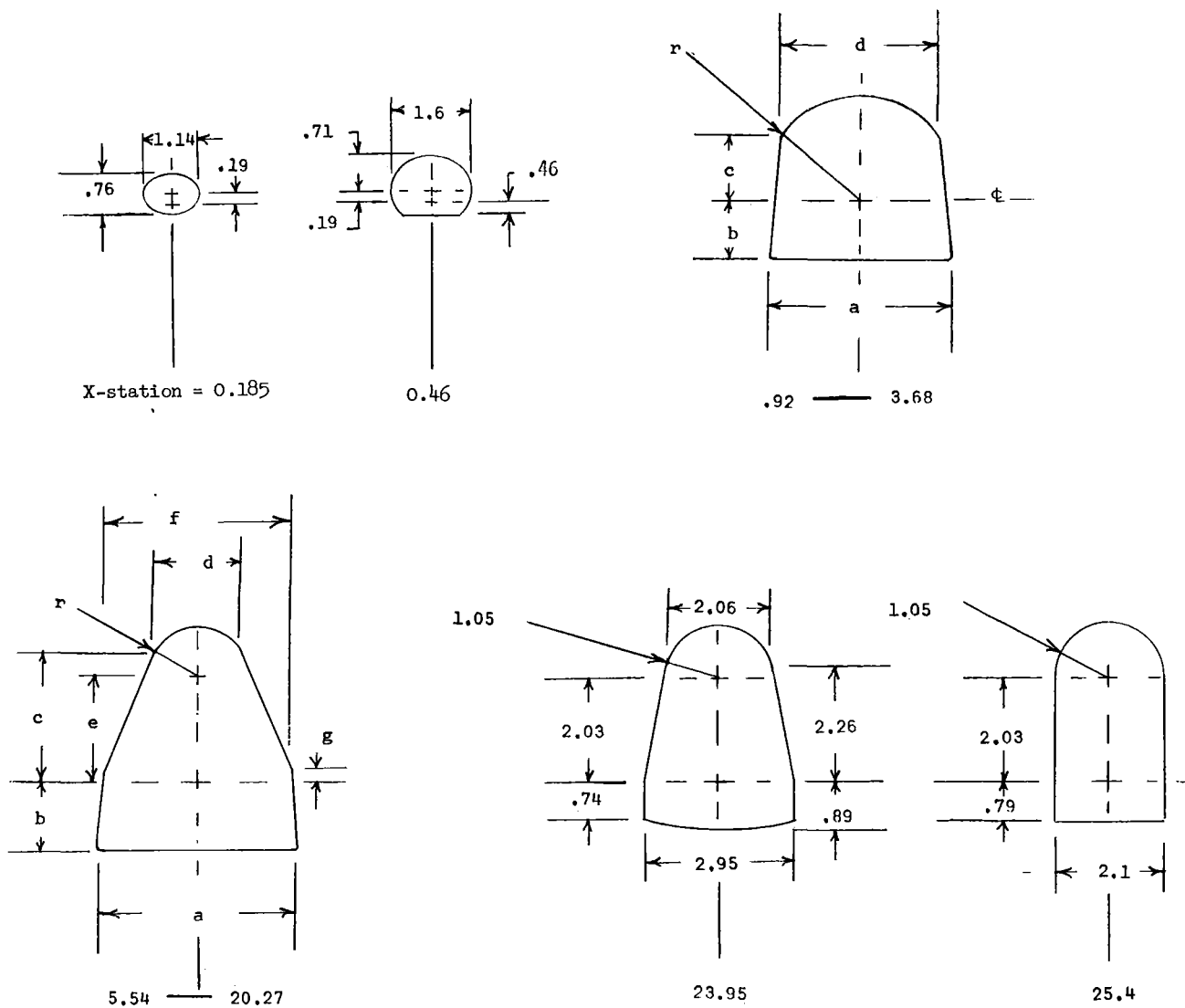
x/c	y/c
Horizontal tail (NACA 0012-64); center-line root chord, 2.98; tip chord, 1.05	
0.10	0.04
.40	.06
.80	.03
1.00	.001
Leading-edge radius, 0.06	Leading-edge radius, 0.02
Vertical tail (NACA 0012-64)	
z = 1.24; c = 6.12	z = 6.48; c = 2.21
0.10	0.04
.40	.06
.80	.03
1.00	.001
Leading-edge radius, 0.11	Leading-edge radius, 0.04

x/c	y/c
Wing root (NACA 0014-64); center-line root chord, 3.75	
0.15	0.06
.50	.07
.90	.02
1.00	.002
Leading-edge radius, 0.06	
Wing tip (NACA 0010-64); tip chord, 1.33	
0.15	0.05
.50	.05
.90	.01
1.00	.005
Leading-edge radius, 0.02	



(a) General arrangement.

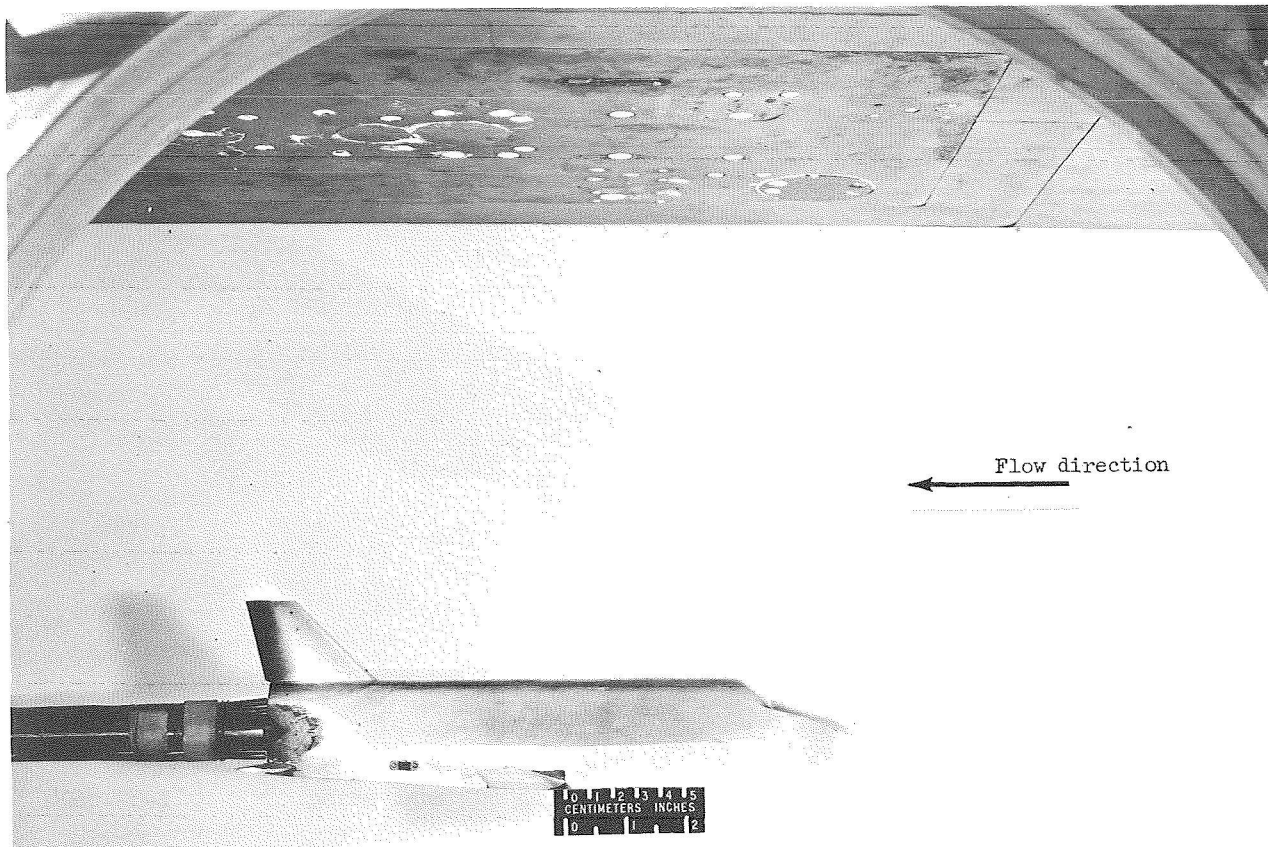
Figure 1.- Details of model. All linear dimensions are in centimeters.



X-station	a	b	c	d	e	f	g	r
0.92	2.22	0.46	0.66	1.93				1.14
1.85	2.79	.73	1.02	2.11				1.47
2.76	3.25	.97	1.12	2.62				1.78
3.68	3.56	1.14	1.27	3.05				2.03
5.54	3.91	1.37	2.41	1.75	2.03	3.68	0.25	.99
7.37	4.06	1.42	2.49	1.91	2.03	3.81	.25	1.05
11.05	4.19	1.52	2.49	1.91	2.03	3.94	.29	1.05
13.82	4.14	1.63	2.49	1.91	2.03	3.94	.29	1.05
15.55	3.94	1.52	2.48	1.91	2.03	3.94	.29	1.05
20.27	3.94	1.21	2.48	1.91	2.03	3.94	.29	1.05

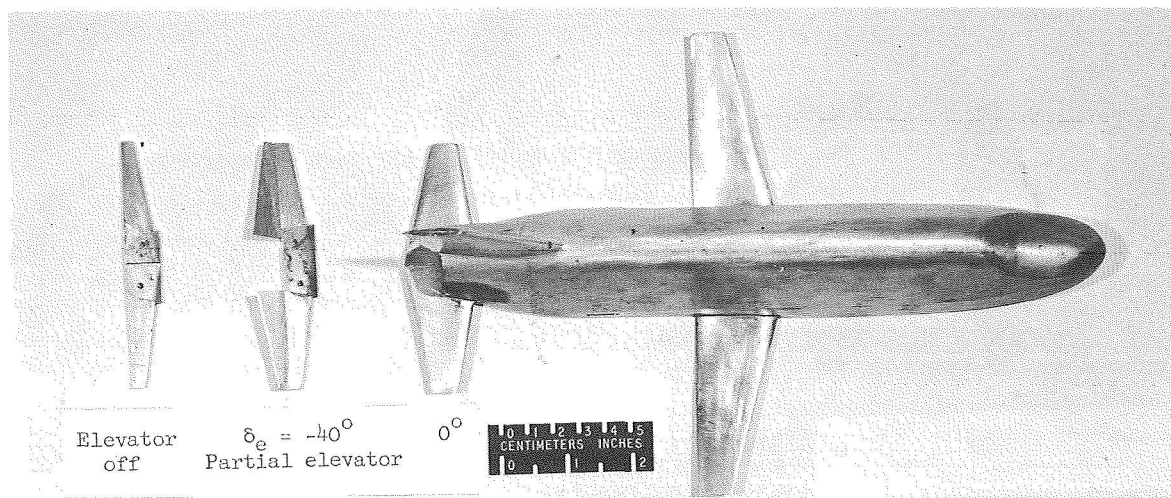
(b) Cross sections.

Figure 1.- Concluded.



(a) Side view of model in tunnel using straight sting.

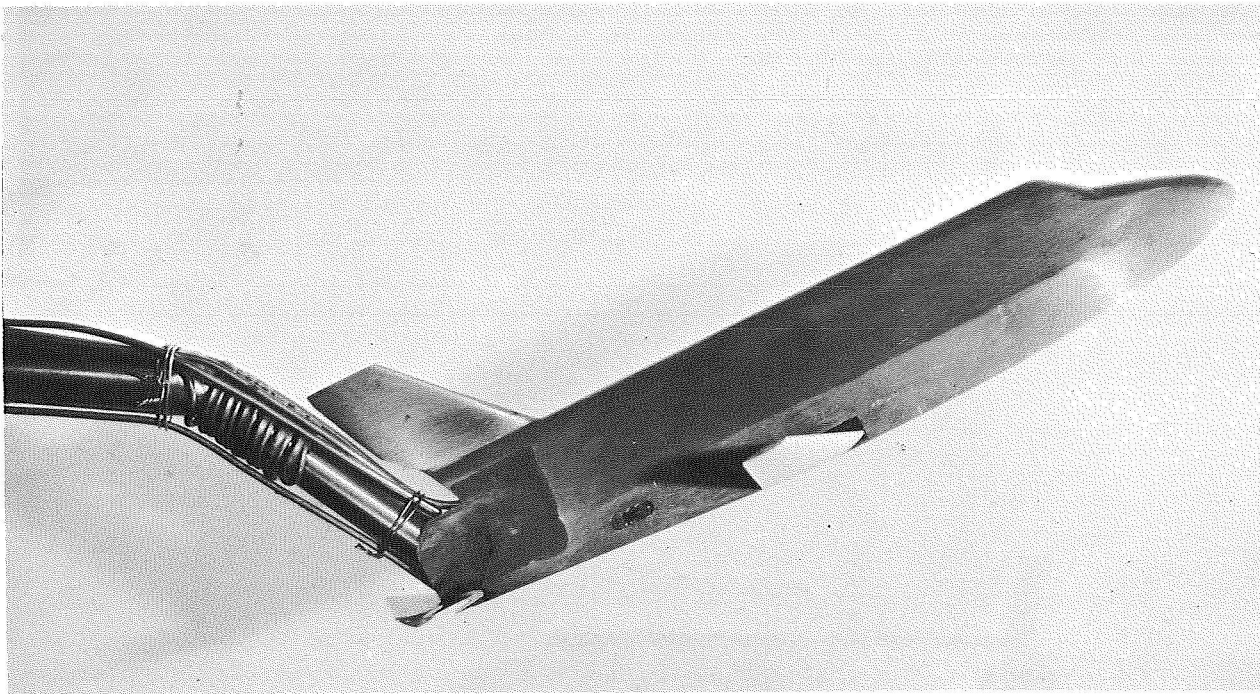
L-69-7484.1



(b) Model and horizontal tails used with straight sting.

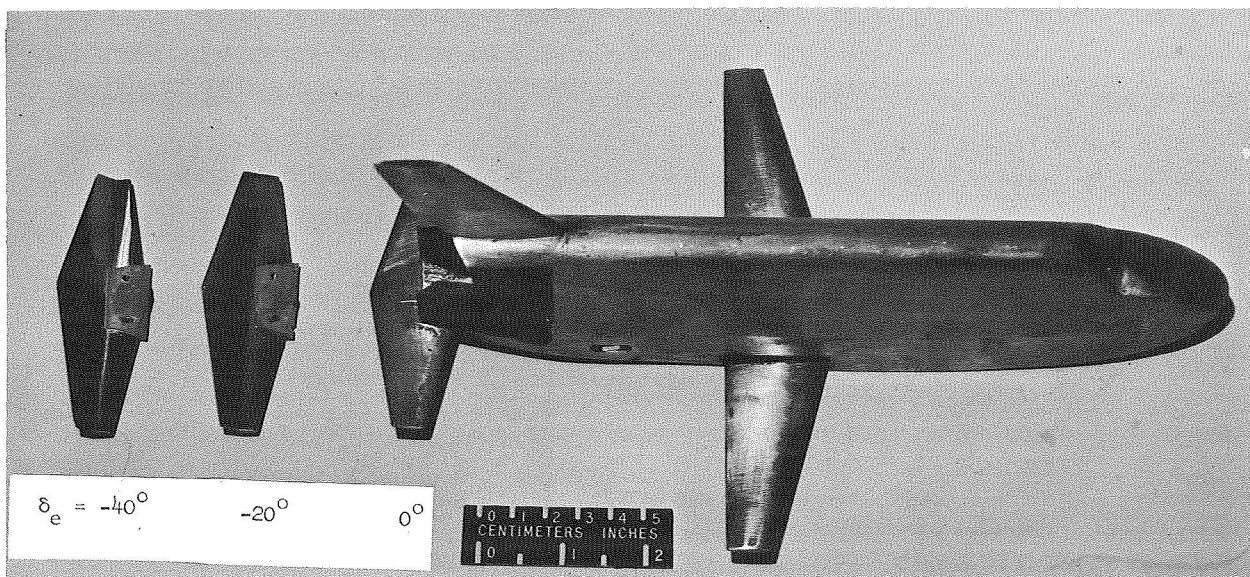
L-69-7478.1

Figure 2.- Photographs of model and horizontal tails used for each sting arrangement.



(c) Side view of model in tunnel using 60° bent sting.

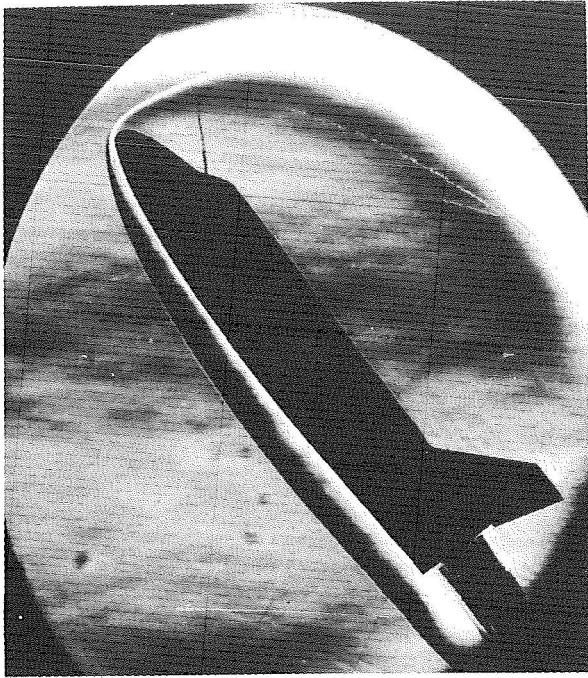
L-69-8624



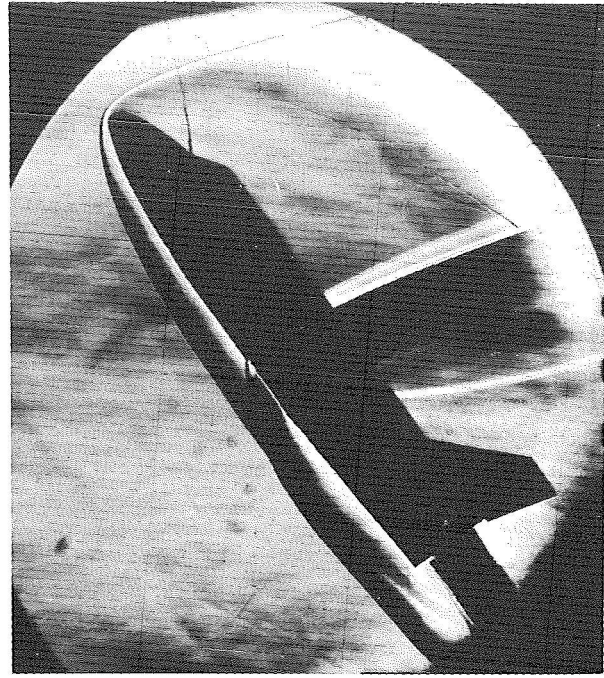
(d) Model and horizontal tails used with 60° bent sting.

L-69-8623.1

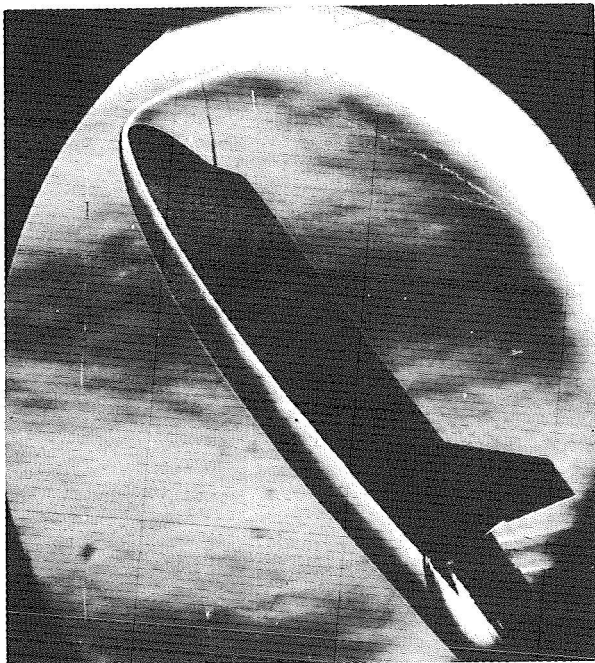
Figure 2.- Concluded.



(a)  $B_1V_3$ .



(b)  $B_1V_3W_2$ .



(c)  $B_1V_3H_6$ ;  $\delta_e = 0^\circ$ .

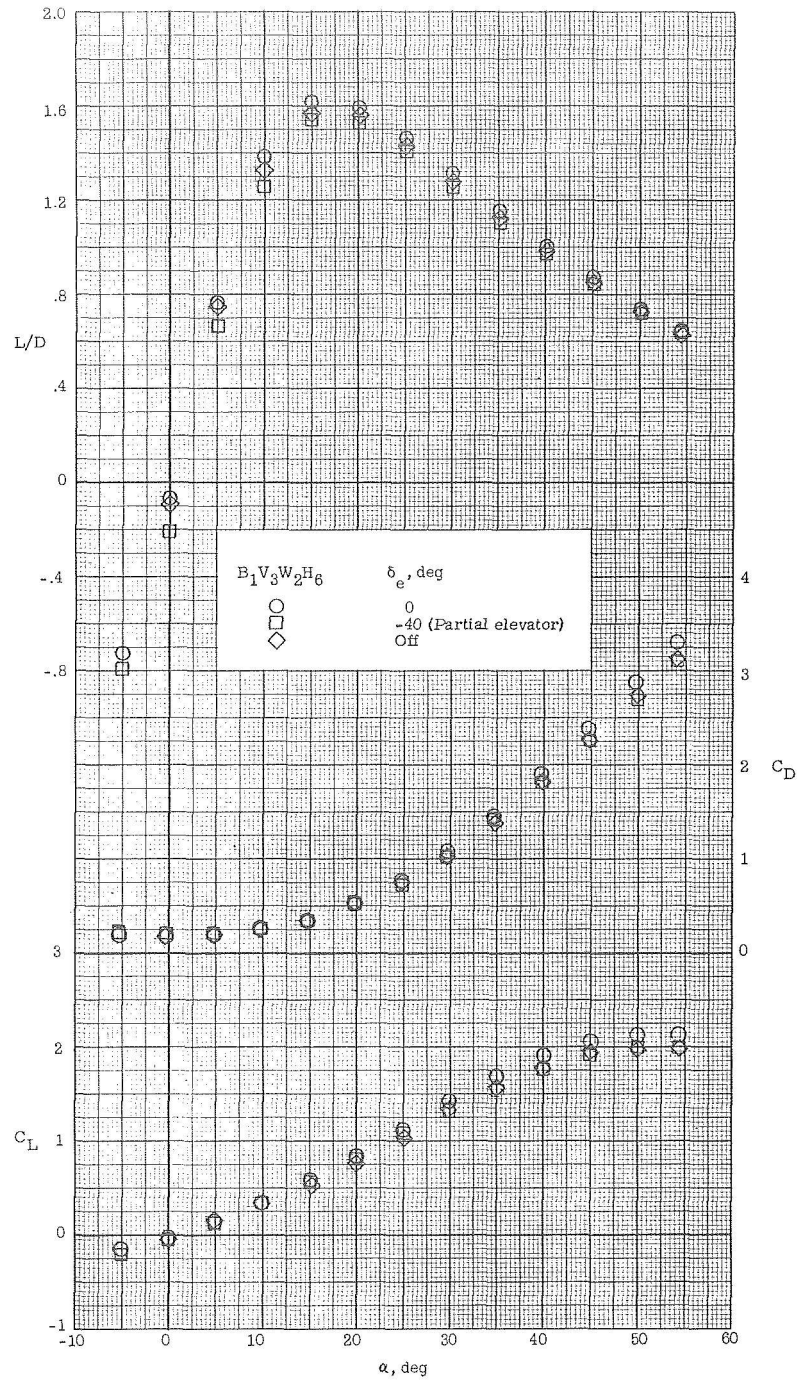


(d)  $B_1V_3H_6$ ;  $\delta_e = 0^\circ$ .

L-70-4742

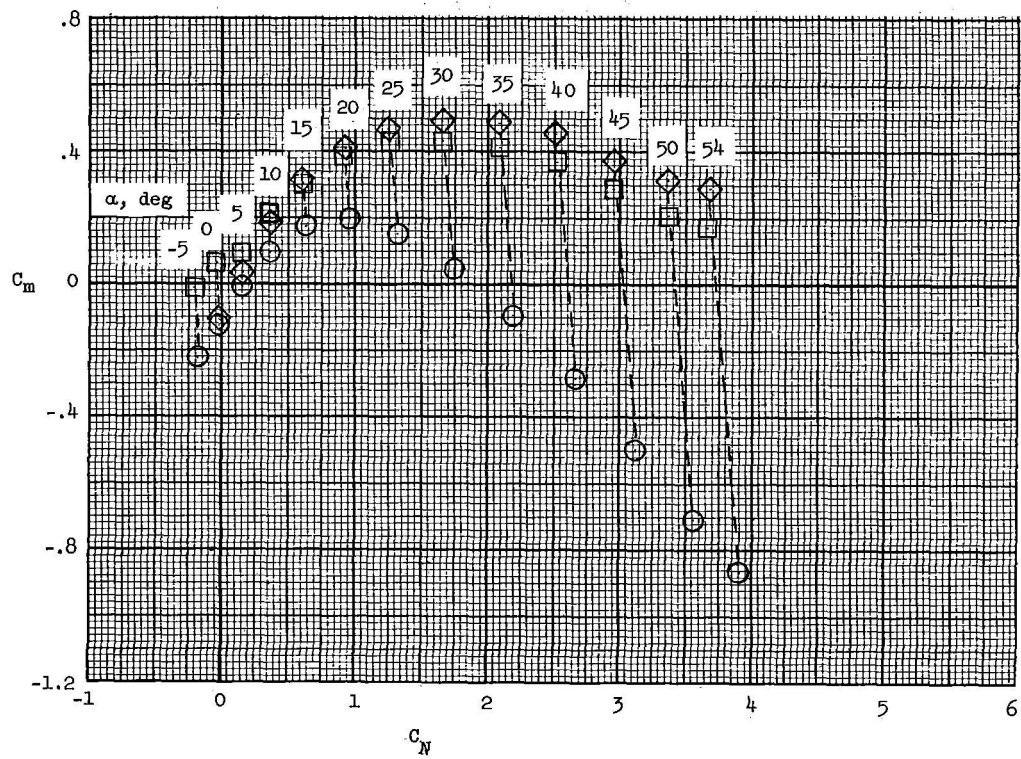
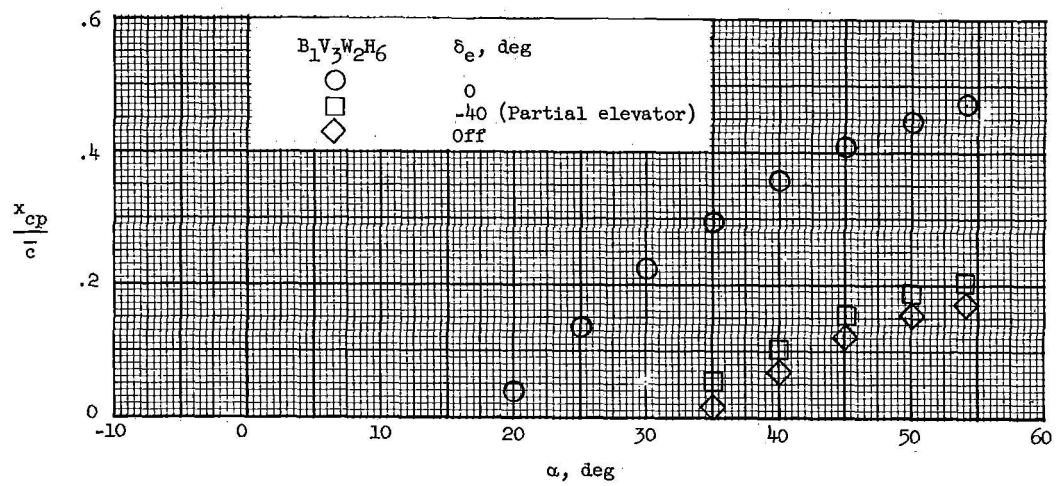
Figure 3.- Schlieren photographs indicating some of the shock structure for the body buildup.  $\alpha = 54.2^\circ$ .





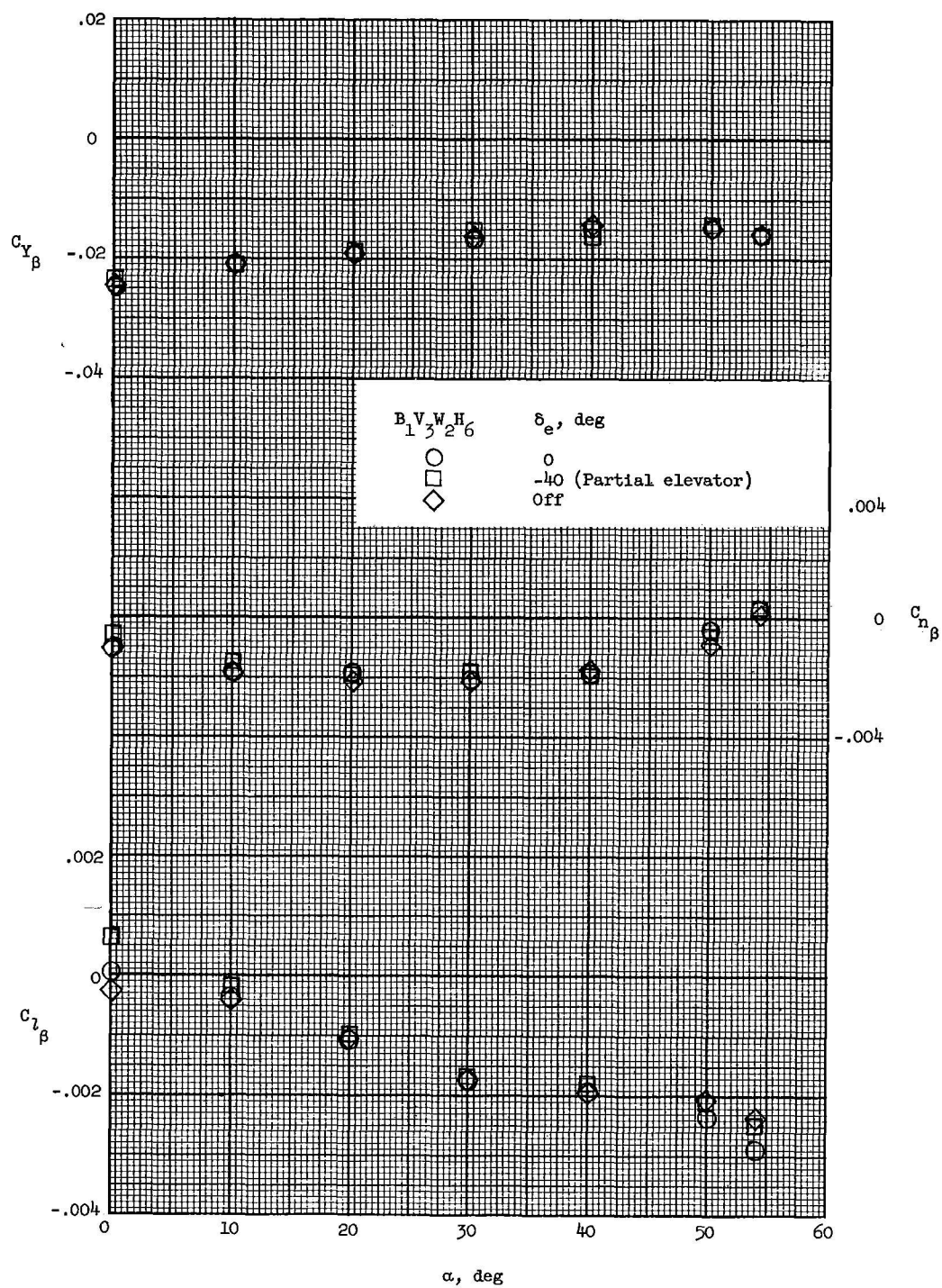
(a) Longitudinal force characteristics.

Figure 4.- Longitudinal, lateral, and directional stability characteristics for various elevator deflections obtained by using the straight sting.



(b) Longitudinal stability characteristics.

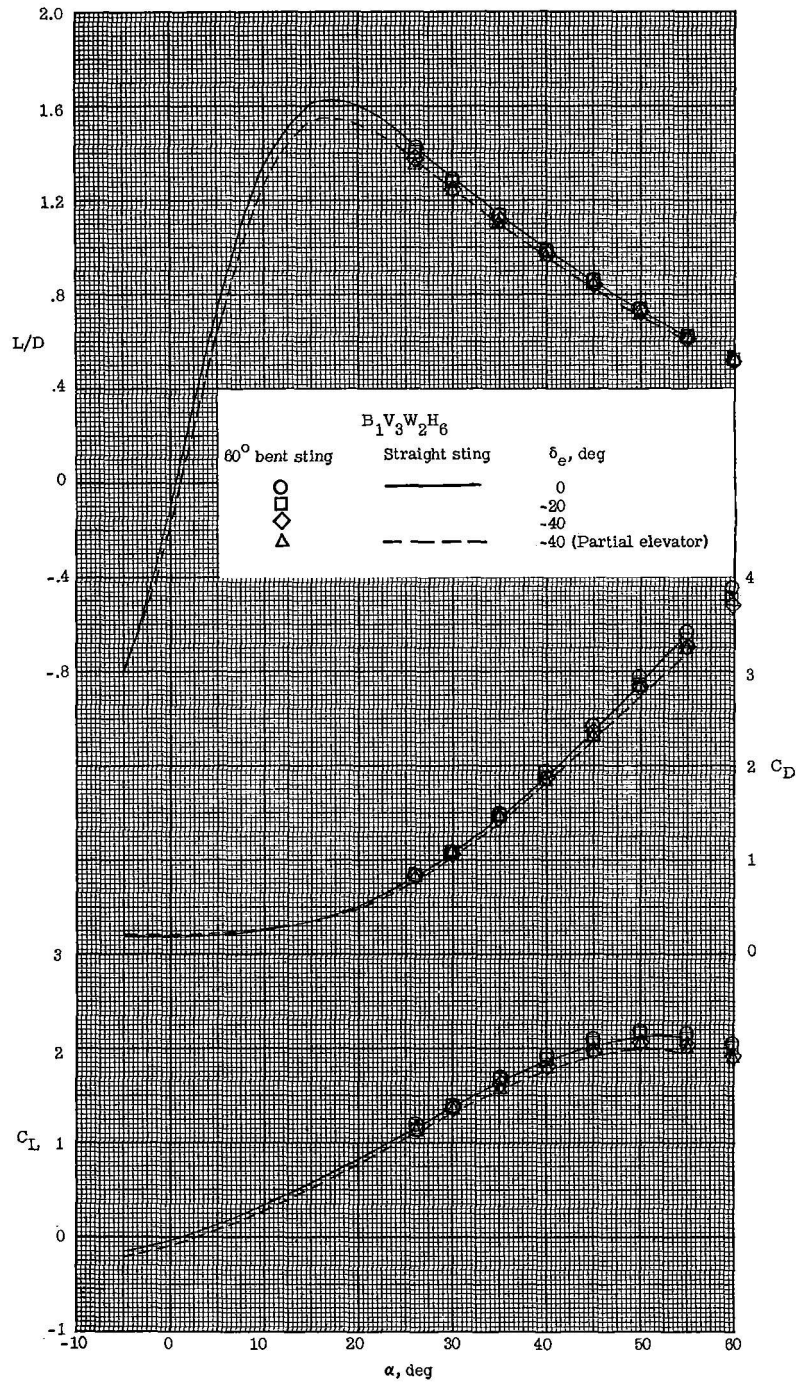
Figure 4.- Continued.



(c) Lateral and directional stability characteristics.

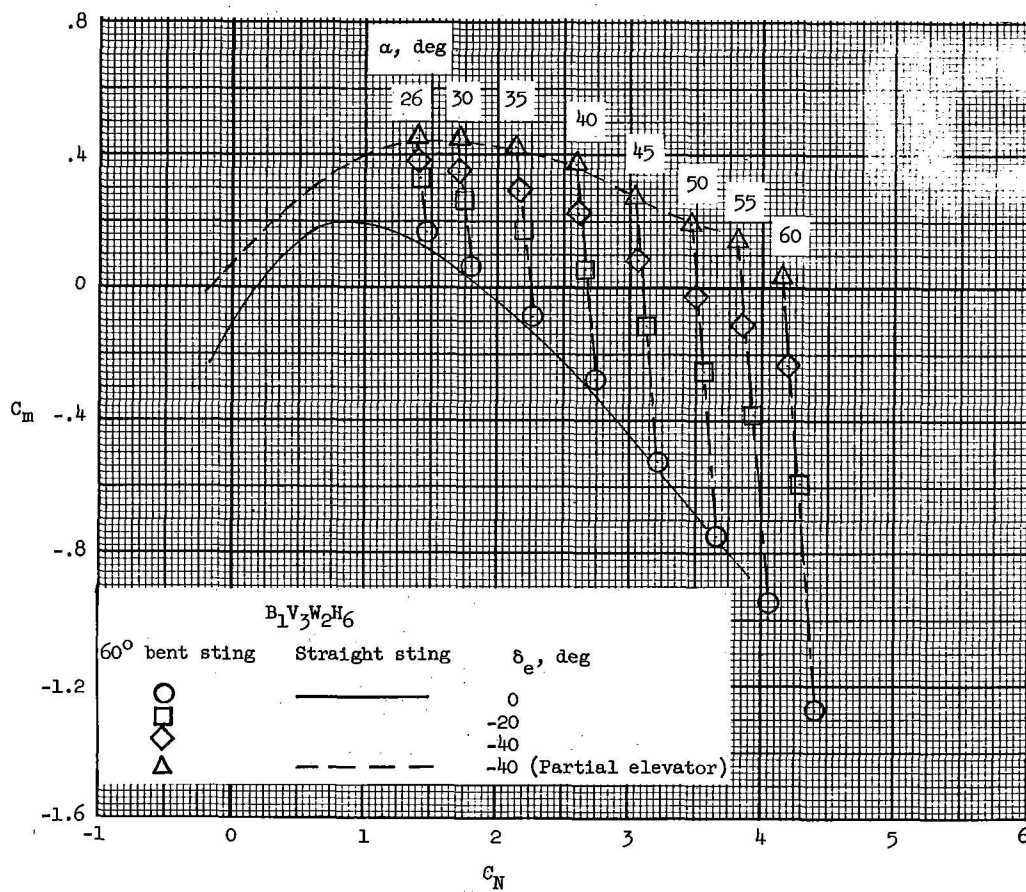
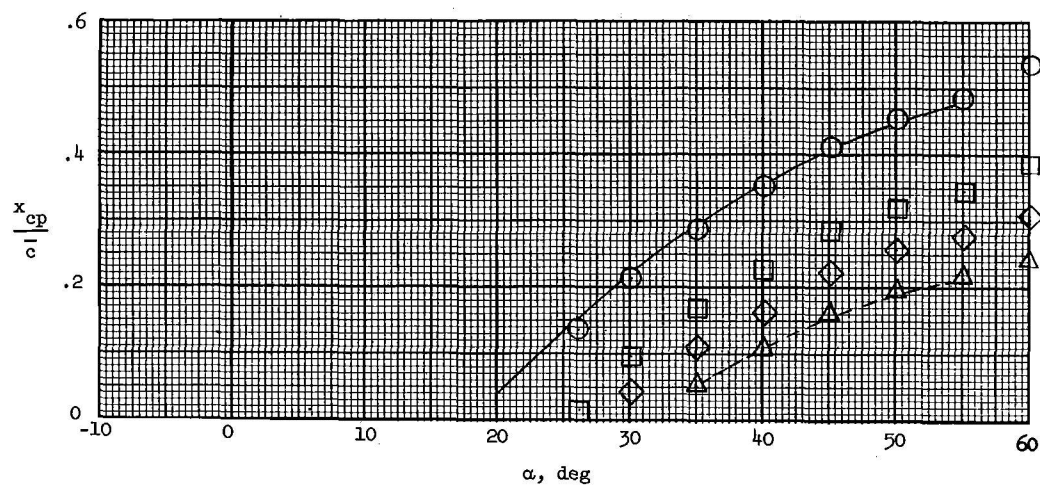
Figure 4.- Concluded.





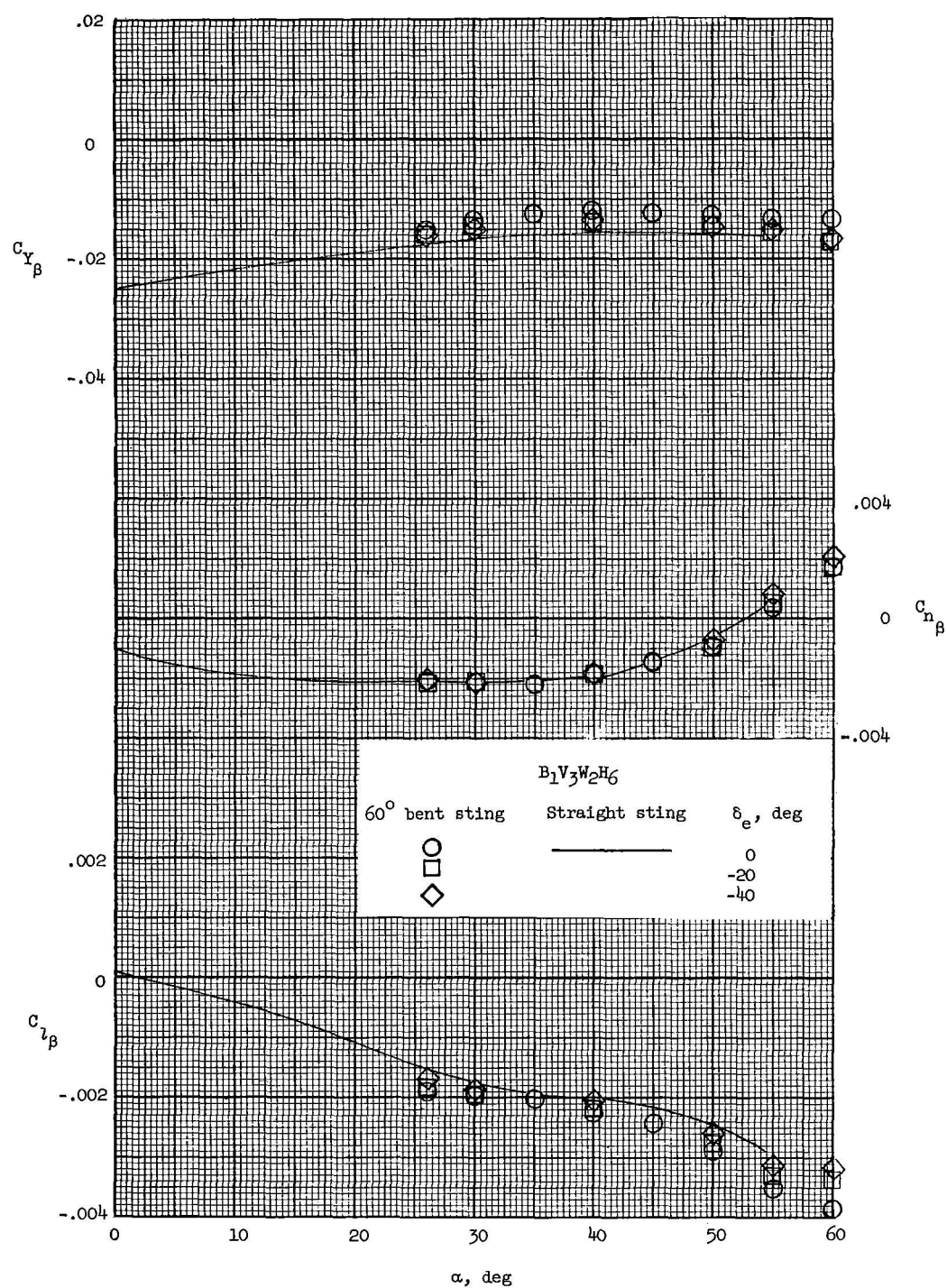
(a) Longitudinal force characteristics.

Figure 5.- Longitudinal, lateral, and directional stability characteristics for various elevator deflections obtained on the 60° bent sting with a comparison to the straight-sting data.



(b) Longitudinal stability characteristics.

Figure 5.- Continued.



(c) Lateral and directional stability characteristics.

Figure 5.- Concluded.

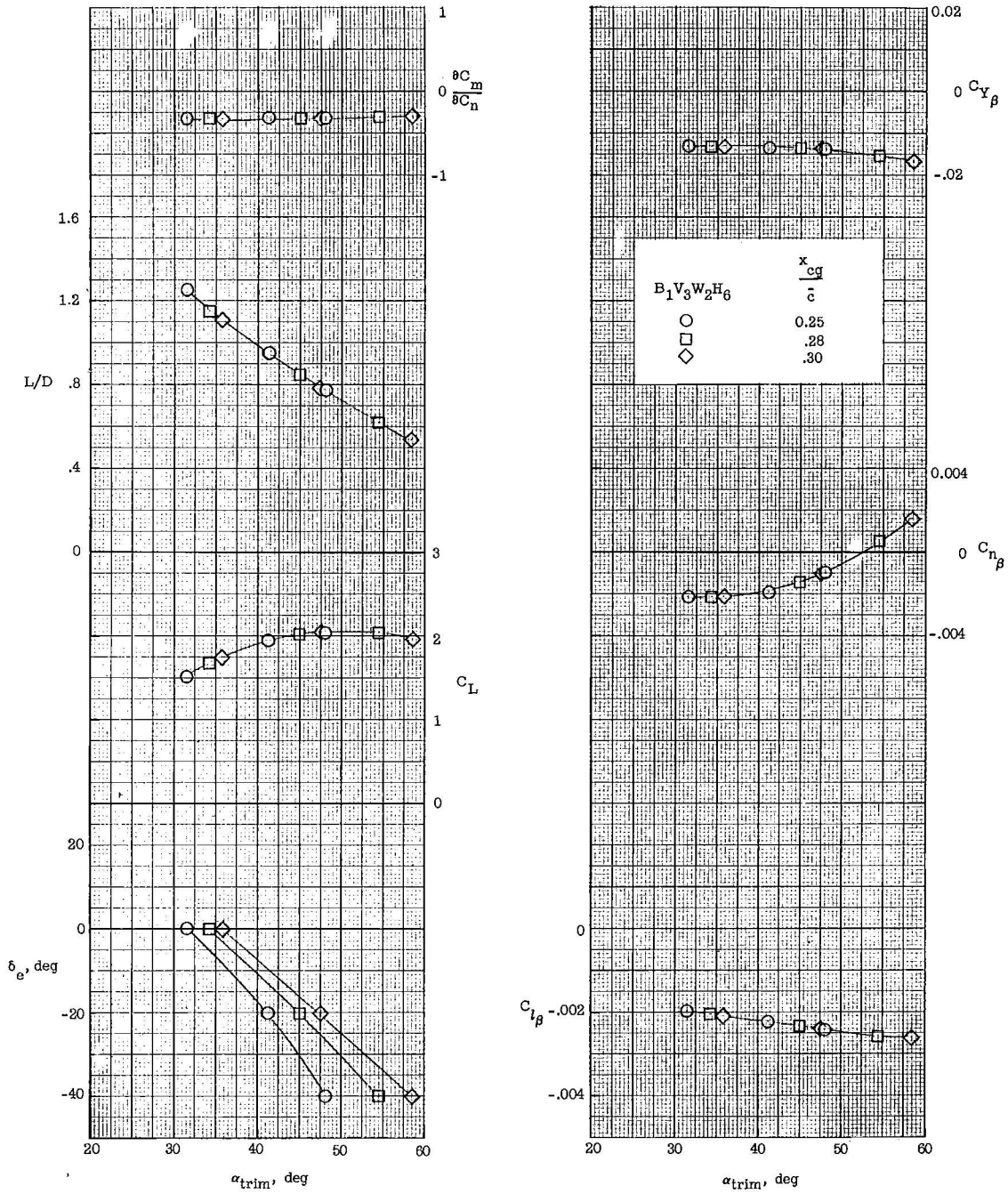
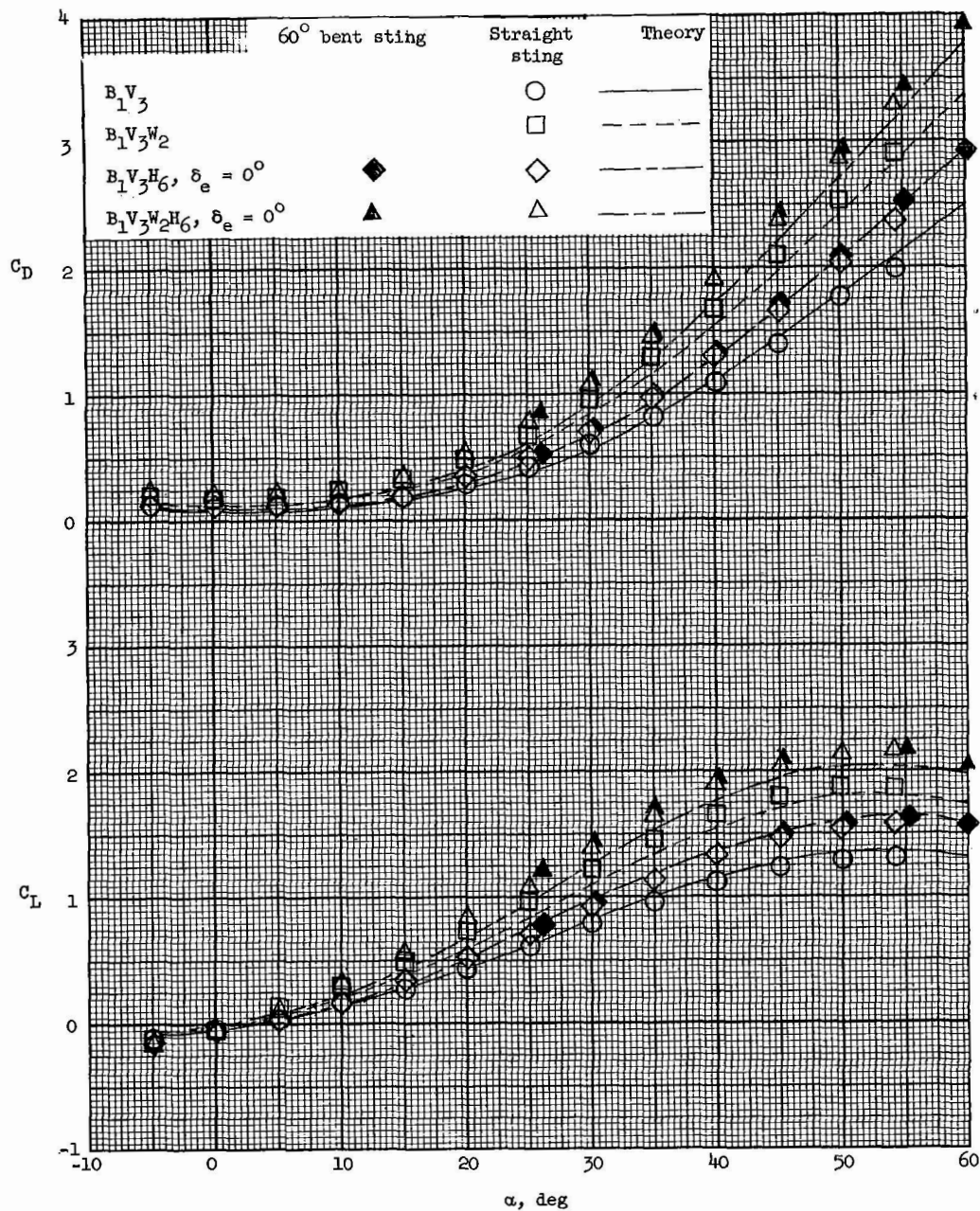


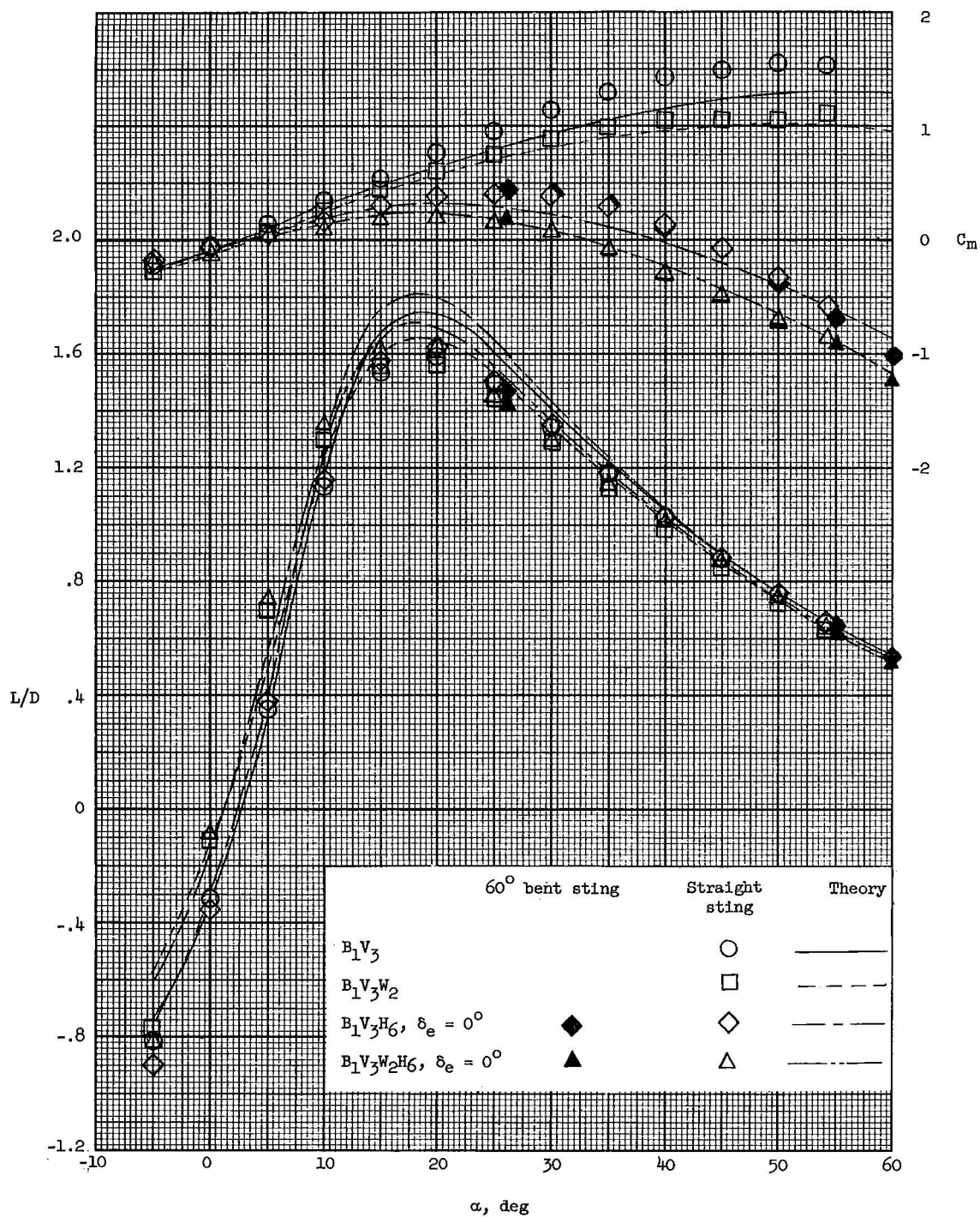
Figure 6.- Longitudinal, lateral, and directional stability characteristics at trim condition for the baseline configuration and using the 60° bent sting.



(a)  $C_L$  and  $C_D$ .

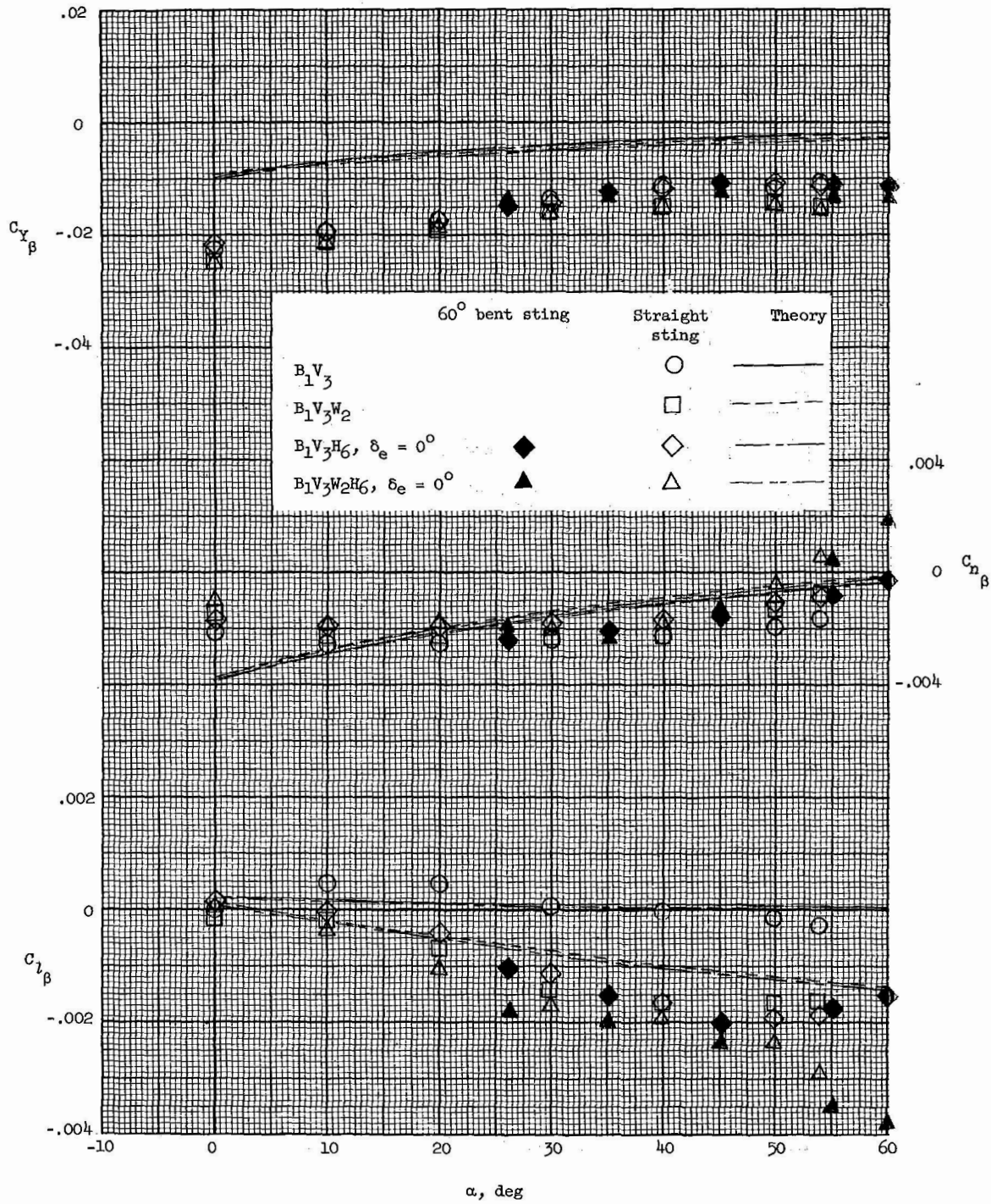
Figure 7.- Longitudinal, lateral, and directional characteristics for configuration buildup and comparison with modified Newtonian theory.





(b)  $L/D$  and  $C_m$ .

Figure 7.- Continued.



(c) Lateral and directional stability characteristics.

Figure 7.- Concluded.

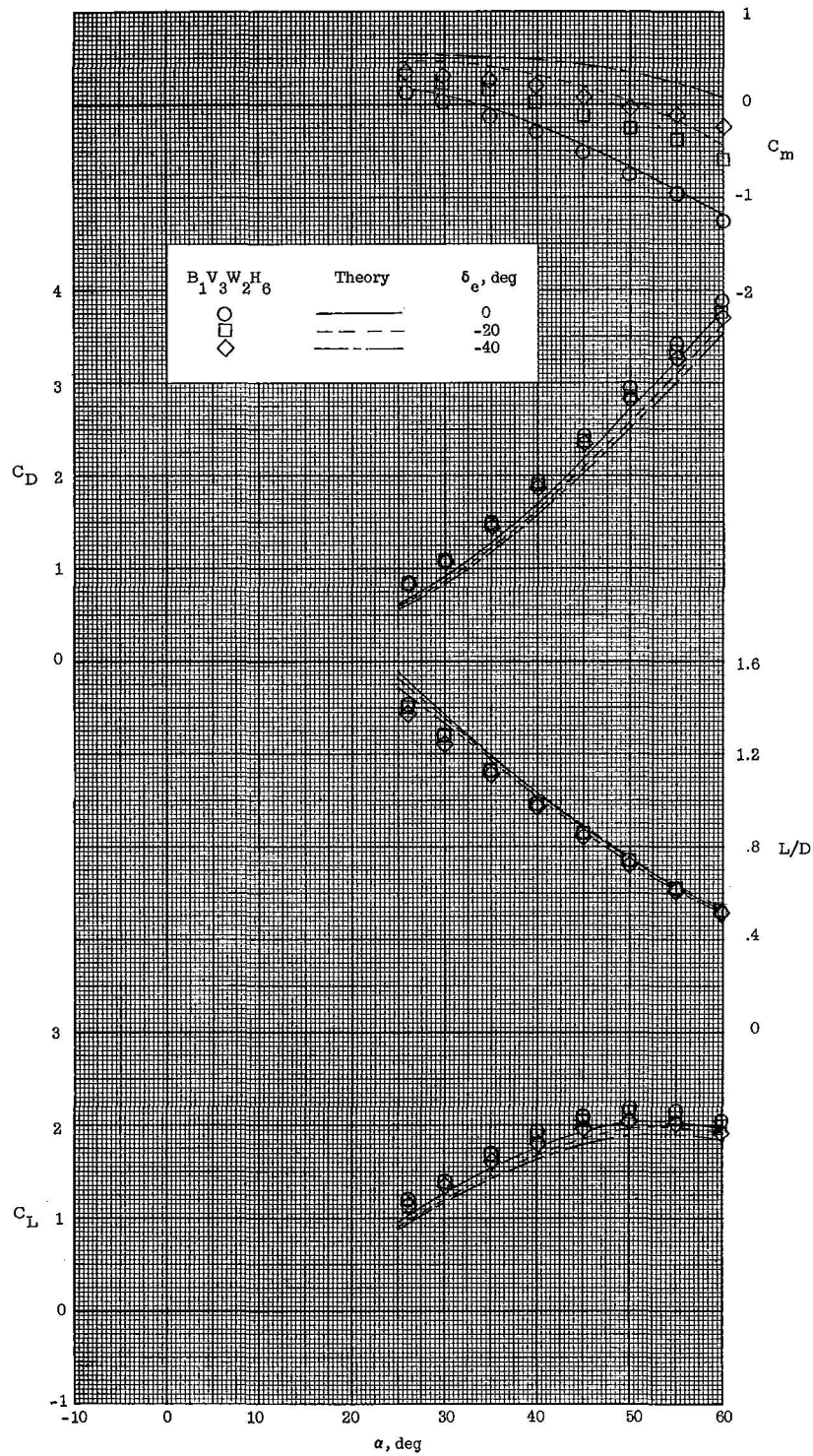


Figure 8.- Longitudinal aerodynamic characteristics of baseline configuration with elevator deflections and a comparison with modified Newtonian theory.





POSTAGE AND FEES PAID  
NATIONAL AERONAUTICS AND  
SPACE ADMINISTRATION

POSTMASTER: If Undeliverable (Section 158  
Postal Manual) Do Not Return

*"The aeronautical and space activities of the United States shall be conducted so as to contribute . . . to the expansion of human knowledge of phenomena in the atmosphere and space. The Administration shall provide for the widest practicable and appropriate dissemination of information concerning its activities and the results thereof."*

— NATIONAL AERONAUTICS AND SPACE ACT OF 1958

## NASA SCIENTIFIC AND TECHNICAL PUBLICATIONS

**TECHNICAL REPORTS:** Scientific and technical information considered important, complete, and a lasting contribution to existing knowledge.

**TECHNICAL NOTES:** Information less broad in scope but nevertheless of importance as a contribution to existing knowledge.

**TECHNICAL MEMORANDUMS:** Information receiving limited distribution because of preliminary data, security classification, or other reasons.

**CONTRACTOR REPORTS:** Scientific and technical information generated under a NASA contract or grant and considered an important contribution to existing knowledge.

**TECHNICAL TRANSLATIONS:** Information published in a foreign language considered to merit NASA distribution in English.

**SPECIAL PUBLICATIONS:** Information derived from or of value to NASA activities. Publications include conference proceedings, monographs, data compilations, handbooks, sourcebooks, and special bibliographies.

**TECHNOLOGY UTILIZATION PUBLICATIONS:** Information on technology used by NASA that may be of particular interest in commercial and other non-aerospace applications. Publications include Tech Briefs, Technology Utilization Reports and Notes, and Technology Surveys.

*Details on the availability of these publications may be obtained from:*

SCIENTIFIC AND TECHNICAL INFORMATION DIVISION  
NATIONAL AERONAUTICS AND SPACE ADMINISTRATION  
Washington, D.C. 20546